JOURNAL OF CHEMICAL INFORMATION AND MODELING

Article

pubs.acs.org/jcim

Conformational Preferences of Modified Uridines: Comparison of AMBER Derived Force Fields

Indrajit Deb,[†] Joanna Sarzynska,[‡] Lennart Nilsson,[§] and Ansuman Lahiri*[,†]

[†]Department of Biophysics, Molecular Biology & Bioinformatics, University of Calcutta, Kolkata 700009, West Bengal, India

[‡]Department of Bioinformatics, Institute of Bioorganic Chemistry, Polish Academy of Sciences, Poznan 61-713, Poland

[§]Department of Biosciences and Nutrition, Centre for Biosciences, Karolinska Institutet, Huddinge SE-141 57, Sweden

Supporting Information

ABSTRACT: The widespread occurrence of modified residues in RNA sequences necessitates development of accurate parameters for these modifications for reliable modeling of RNA structure and dynamics. A comprehensive set of parameters for the 107 naturally occurring RNA modifications was proposed by Aduri et al. (*J. Chem. Theory Comput.* **2007**, *3*, 1464−1475) for the AMBER FF99 force field. In this work, we tested these parameters on a set of modified uridine residues, namely, dihydrouridine, 2-thiouridine, 4-thiouridine, pseudouridine, and uridine-5-oxyacetic acid, by performing molecular dynamics and replica exchange molecular dynamics simulations of these nucleosides. Although our simulations using the FF99 force field did not, in general, reproduce the experimentally observed conformational characteristics well, combination of the parameter set with recent revisions of the FF99 force field for RNA showed noticeable improvement for some of the nucleosides.

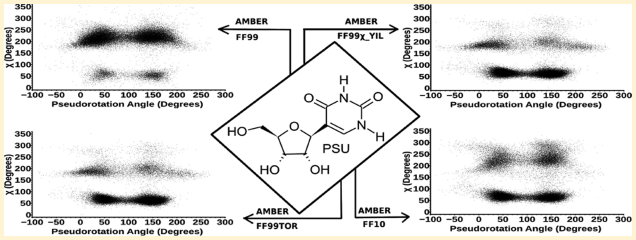

INTRODUCTION

A characteristic feature of RNAs, especially tRNAs, is the ubiquitous occurrence of modified residues. According to the latest update of the RNA modification database (RNAMDB) which provides a comprehensive listing of post-transcriptionally modified ribonucleosides, 109 such modifications have been so far characterized.[1] Another useful repository of information about the chemical structure of naturally occurring RNA modifications, their location in RNA, and their synthesis pathway is MODOMICS.[2] The frequency of occurrence of modifications can be quite high, particularly for tRNAs. Analysis of 561 tRNA sequences has revealed 11.9% of the residues to be modified.[3,4] In tRNA, the modifications are distributed throughout the sequence, although the four stem regions are relatively modification free, with modifications preferring the junction regions between stems or loops. There are a number of instances where the presence and absence of modifications lead to large structural changes.[5−11] Significant alteration of secondary structure and alternative folding have been observed, for example, due to the presence of one or several modifications.[8] However, many of the modifications seem to be responsible for more subtle effects acting in coordination with other modifications to give rise to the desired functionality of the tRNA. Ribosomal RNAs (rRNAs) also show the presence of modified residues. The modified residues in rRNAs occur mostly in regions that play important functional roles in ribosomal subunit association, tRNA and mRNA recognition, and formation of peptide bond.[12,13] Various aspects of RNA modifications have been recently reviewed.[14−16]

Our understanding of the functionality of these modifications is still evolving.[17] Generally, these modifications are seen as an additional layer of chemical diversity that enhances the information coding capacity of the four standard nucleic acid residues (A, C, G. and T/U for DNA/RNA, respectively).[16] For DNA, where the diversity of modifications is much less than in RNA, the modifications are thought to carry information about lesions and epigenetic information.[16] On the other hand, the large diversity of modifications in RNA is consistent with the multifarious biological roles it plays in addition to being an information carrier.[8]

For tRNA, an attempt to classify the modifications on the basis of their functions has led to three broad groups[16] of which the group pertaining to the modifications occurring in or around the anticodon contains the largest diversity of modifications. Conceivably, these modifications are involved in what is purported to be the major function of tRNA, i.e., decoding the codons provided by mRNAs. Surprisingly, a recent high resolution crystal structure of a completely unmodified *E. coli* $tRNA^{Phe}$ has revealed unexpectedly little structural differences compared with the native structure.[18] This implies that apart from causing large scale changes in the RNA structure, the effect of modifications can also be quite subtle. In fact, experimental evidence[19−23] points to an alteration of local rigidity or flexibility of the anticodon as a result of occurrence or absence of modifications in or around it.

Received: October 8, 2013
Published: April 3, 2014

Modeling these effects accurately encompassing all the chemical diversity has thrown up an immense challenge for molecular modelers. In fact, even a decade back, force field parameters were available only for a handful of these modifications[20,24−29] (http://www.pharmacy.manchester.ac.uk/bryce/amber/). This deficiency was first systematically addressed by the work of Aduri et al.[30] where they provided a parameter set for all the 107 naturally occurring RNA modifications known at the time consistent with the present AMBER FF99 force field[31] which has been derived from the Cornell et al. force field[32] of AMBER. As of now, this is the most comprehensive source of parameters for researchers interested in modeling the structural or dynamical consequences of RNA modifications.

However, although great effort was made in the Aduri et al.[30] force field to make it consistent with the FF99 force field, a potential drawback of the force field was that it was never systematically tested and validated by comparing simulation results with experimental data. This assumed more pertinence as subsequent investigations brought to the fore the deficiencies in the FF99 force field itself.[33−41]

As a result of current intense activity by several groups, a number of revisions of the AMBER force field parameters has been put forward.[33,34,36,39−41] Many of these revisions are focused on the reparameterization of different torsional parameters.[33,34,36,39,40] In a recent work, Chen and Garcia have additionally reoptimized the Lennard-Jonnes parameters along with the glycosidic torsion parameters (χ) for obtaining accurate folding of RNA tetraloops.[41] These developments prompted us to study i) how accurate are the Aduri et al. parameters in the context of its original FF99 force field and ii) does the combination of this parameter set with the modern revisions of FF99[33,36,39,40] provide a better description of the conformation of modified RNA residues. We report here the results of molecular dynamics simulations that address these issues for the modified uridine nucleosides dihydrouridine (DHU), pseudouridine (PSU), 2-thiouridine (2SU), 4-thiouridine (4SU), and uridine-5-oxyacetic acid (OAU) (Figure 1). As pointed out earlier,[36] ribonucleosides as test systems have been generally neglected in benchmarking AMBER force fields. However, validating force fields through simulation of nucleosides has its advantages in comparison with oligonucleotide test systems since it is much easier to achieve convergence with the former leading to a more accurate picture of the equilibrium conformational distributions.

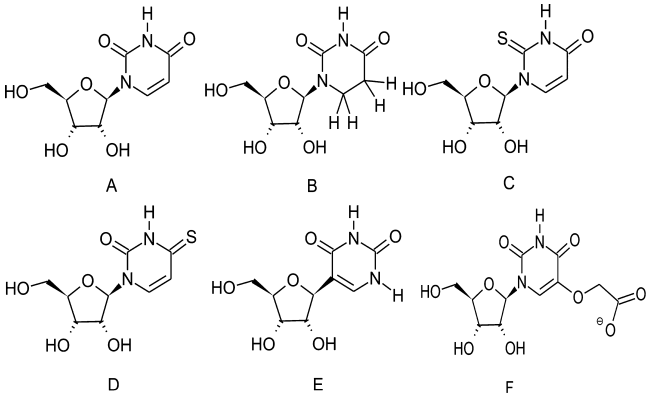

Figure 1. Nucleosides studied in this work: A. uridine (U), B. dihydrouridine (DHU), C. 2-thiouridine (2SU), D. 4-thiouridine (4SU), E. pseudouridine (PSU), and F. uridine-5-oxyacetic acid (OAU).

Among the ribonucleosides studied in the present work, the first three modifications are found in all three domains of life, while 4-thiouridine is found in both bacteria and archaea and uridine-5-oxyacetic acid being observed only in bacteria.[16]

Dihydrouridine (DHU) is one of the most common modifications occurring in tRNAs of eukaryotes and bacteria. It is also one of the most conserved modified nucleosides in tRNA, mainly occurring in the D loop and sometimes in the variable loop.[42,43] Structurally, dihydrouridine has the C5−C6 bond saturated as a result of which the base ring loses its planarity. This is supposed to cause significant consequence to the structural stability of strands/structures containing dihydrouridine resulting in increased flexibility to the molecule. The modification also drives the sugar pucker which is slightly favorable to C3′-endo in uridine to a strongly C2′-endo favoring conformation.

2-Thiouridine occurs mostly at the wobble position. Dihydrouridine and 2-thiouridine exemplify two extreme cases of conformational preferences with dihydrouridine preferring the C2′-endo conformation and 2-thiouridine preferring the C3′-endo conformation.

Pseudouridine (5-ribosyluracil) is again one of the most common modifications in RNA and the first of the modified residues to be discovered ("the fifth nucleoside").[44] Its distinctive characteristic of having a C−C instead of an N−C glycosyl bond is thought to result in increased rotational freedom. In general, pseudouridine is considered to possess more conformational flexibility than uridine. The free nucleoside also has a slight preference for a SYN conformation as compared to the preference for ANTI in the case of uridine.[45−47]

Another well-characterized tRNA modification is 4SU which occurs at position 8 of tRNA. It carries a thio modification at C4 of the uracil base and acts as a photosensor in the near-UV range.[48] Exposure to near UV radiation drives a cycloaddition reaction involving 4SU at position 8 and a cytosine at position 13 of the tRNA. The effect of this is a conformation change preventing aminoacylation of the tRNA. A comparative NMR study of U and 4SU suggests a slightly higher preference for the NORTH population for 4SU over U. Although NMR experiments in aqueous solution on 4SU found a predominant population of the ANTI conformation, X-ray studies observed the SYN conformation in the crystalline state.[49,50]

The nucleoside OAU is notable for its remarkable capacity of being able to read all of the four nucleotides at the wobble position.[51−53] From proton NMR studies, the population of NORTH and SOUTH conformers of OAU appears to be close to that of uridine.[54] The crystal structure of the methyl ester of OAU was found to be in the NORTH conformation.[55] Interestingly, the nucleotide 5-carboxymethoxyuridine 5′-monophosphate (pcmo5U) has a pronounced preference for the SOUTH conformation compared to OAU.[54]

As apparent from the above, the uridine derivatives studied in this work show varied conformational features and, therefore, provide an excellent test system for force field evaluation.

METHODS

Computational Details. All molecular mechanics and dynamics calculations for uridine and its derivatives were performed with the molecular modeling suite AMBER10[56] and AMBER12.[57] The initial structure for the standard nucleoside

Table 1. Comparison of the Latest AMBER Derived Force Fields

variants of AMBER force fields[32]	revised torsions	definition	applied revised torsional terms for the systems under study
FF99[31]	none	The default AMBER FF99 force field parameters for U and Aduri et al. parameters[30] for modified uridines.	not applicable
FF99χ_YIL[36]	χ	The AMBER FF99χ_YIL force field revised by Yildirim et al.[36] It is the combination of AMBER FF99 force field parameters with revised χ torsion parameters.	Revised χ parameters developed by Yildirim et al. (χ_YIL).[36]
FF99TOR[40]	$\chi\alpha\gamma\varepsilon\zeta\beta$	The AMBER FF99 force field with revised α, β, χ, ε, ζ, and χ torsions.[40] Combination of FF99χ_YIL force fields (revised Yildirim et al.[36]) and parmbsc0 (revised α/γ by Perez et al.[33]) as well as reparameterized ε, ζ, and β torsional parameters by Yildirim et al.[40]	Revised χ parameters of Yildirim et al. (χ_YIL)[36] in combination with revised γ parameters of Perez et al.[33]
FF10[39]	$\chi\alpha\gamma$	AMBER FF99 with revised χ torsion parameters developed by Zgarbova et al.[39] in combination with parmbsc0 revised by Perez et al.[33]	Revised χ parameters of Zgarbova et al. (χOL)[39] in combination with revised γ parameters of Perez et al.[33]

uridine was created using the online server http://structure.usc.edu/make-na/server.html, and the PDB files corresponding to their quantum mechanically optimized geometry provided by Aduri et al.[30] along with topology and parameter files for modified RNAs were taken as the starting structures for the uridine derivatives. The tLEAP module embedded within the AMBER program was used to add hydrogens, neutralize, and solvate the systems with TIP3P[58] water molecules in a truncated octahedral solvent box. The three recently revised AMBER force fields - FF99χ_YIL,[36] FF99TOR[40] and FF10[37] (the details of these revised force fields are given in Table 1) - were combined with the parameter set developed by Aduri et al. for 5′-monophosphates of modified uridines. The modified χ and γ parameters were recruited by replacing the atom types describing the χ and γ torsional terms in the original topology files[30] of modified uridines under study with the atom types as defined for these torsional terms in the revised force fields.[36,39,40]

Subsequently the topologies of DHU, 2SU, 4SU, PSU, and OAU nucleosides were generated by substituting the 5′-phosphate group with a hydrogen (5′−OH) atom and adding hydrogen (3′−OH) at the 3′-end in their corresponding topology files. The missing parameters were taken from the FF99 parameter set. The revised force field parameters were developed based on FF99 and were designed for standard residues. The parameter sets for modified RNA residues as developed by Aduri et al.[30] focused on the development of the atom-centered partial charges necessary to compute the electrostatic term in the force field, whereas the force constants and equilibrium distances, bond angles, and dihedral terms not found in FF99 were generated using the general AMBER force field (GAFF).[59] One neutralizing Na+ ion was added to the solvated charged nucleoside OAU. The starting structures of each nucleoside for MD simulations were in a NORTH/ANTI conformation. MD simulations were performed for 200 ns at constant pressure with periodic boundary conditions at 300 K. The 16 ns replica exchange MD (REMD)[60] calculations were carried out at constant volume. In the REMD method, several simulations or replicas of the same system were run at 16 different temperatures spanning a range from 300 K to 400 K, using 16 separate processors. All the MD and REMD simulations were carried out using the SANDER module of the AMBER suite.

MD Simulations. The nucleosides U, DHU, 2SU, 4SU, PSU, and OAU were solvated with TIP3P water molecules in truncated octahedral boxes having 540, 567, 559, 586, 556, and 619 water molecules respectively in a manner so that the closest distance between any atom of the solute and the edge of the periodic box is 9 Å. At first, energy minimization was done by 500 steps of steepest descent followed by 500 steps of conjugate gradient holding the nucleosides restrained with a force of 500 kcal/mol·Å^2. Then all the restraints were removed, and the structures were minimized again by 1000 steps steepest descent followed by 1500 steps conjugate gradient. The nonbonded interactions within 8 Å long-range cutoff were taken into account during minimizations. After minimization, two steps of equilibration were done. In step 1, the nucleosides were heated from 0 K to 300 K in 20 ps with a 2 fs time step using constant volume dynamics with a long-range cutoff of 8 Å holding the nucleosides with a restraint force of 10 kcal/mol·Å^2. Langevin dynamics with random velocity scaling using a collision frequency of 1 ps^{-1} was used. SHAKE[61] was turned on for bonds involving hydrogen atoms. In the second step of equilibration, the above conditions were followed except constant pressure dynamics was used for 200 ps with a 2 fs time step turning on the isotropic position scaling and removing the restraint force applied in step 1. The reference pressure was 1 atm with a pressure relaxation time of 2 ps. The particle mesh Ewald (PME) method[62] was used for all simulations. The production run was similar to the second step of the equilibration described above. For each nucleoside, a total of 200 ns of MD were run with a 1 fs time step. Trajectory files were written at each 10 ps time step for all nucleosides.

Three separate explicit solvent MD simulations of 200 ns each were carried out at 300 K yielding a total of 600 ns for each nucleoside for each force field. Each of the three separate simulations had the same starting structure.

REMD Simulations. In replica exchange MD several simulations or replicas of the same system are run at different temperatures. Temperatures are exchanged between two replicas, i and j, with the probability $P(\text{exchange}) = \exp[-(\beta_i - \beta_j)(E_i - E_j)]$, where $\beta = 1/k_B T$, k_B is the Boltzmann constant, T is the absolute temperature, and E is the potential energy.

REMD calculations in explicit water were carried out using the multisander approach that runs multiple sander jobs concurrently under a single MPI. We simulated sixteen replicas running at temperatures T = 300.0, 305.8, 311.7, 317.8, 323.9, 330.2, 336.6, 343.1, 349.7, 356.5, 363.4, 370.5, 377.6, 384.9, 392.4, and 400.0 K. Constant volume REMD of 2000 cycles consisting of 4000 steps of molecular dynamics with a 2 fs time step followed by attempted exchange between replicas with neighboring temperatures was run, giving 16 ns for each replica and a total of 256 ns of simulation time. Langevin dynamics with random velocity scaling using a collision frequency of 1 ps^{-1} was used. SHAKE[48] was turned on for bonds involving hydrogen atoms during equilibration at target temperature before exchange. The input coordinates for REMD simulation were the final coordinates from the two step equilibration run

Table 2. Percent (%) of NORTH Sugar Puckering Predicted by Various Force Fields Using Both the MD and REMD Simulations and Puckering Determined Experimentally by NMR[a]

	U	DHU	2SU	4SU	PSU	OAU
FF99	33.7(1.1)	24.7(0.6)	33.3(0.6)	22.3(0.6)	49.0(0.0)	51.3(0.6)
	33	*25*	*33*	*22*	*50*	*49*
FF99χ_YIL	54.0(1.0)	40.7(1.5)	40.7(0.6)	31.3(1.2)	48.3(0.6)	65.3(3.8)
	53	*40*	*42*	*28*	*51*	*67*
FF99TOR	46.3(2.1)	49.3(0.6)	47.0(0.0)	37.3(0.6)	40.6(1.2)	63.6(3.8)
	45	*49*	*46*	*37*	*39*	*57*
FF10	40.6(0.6)	47.6(0.6)	42.0(2.6)	33.3(1.2)	46.0(0.0)	55.3(2.1)
	43	*47*	*43*	*33*	*43*	*59*
CHARMM27[b]	64.3[c], 72.2[d]	NA	NA	NA	NA	NA
CHARMM27[e]	70[f],73[g], 54[h]	NA	83[f], 77[g], 89[h]	NA	NA	NA
FF99[i]	35	NA	NA	NA	NA	NA
FF99χ_YIL[i]	55	NA	NA	NA	NA	NA
NMR	54[j], 54[k], 55[l], 53[m],56[n]	32[k], 36[m]	74[l], 71[m]	61[m]	51[m], 50[o]	56[p]

[a]The values reported are the averages calculated from three independent 200 ns MD simulations, and the standard deviations are in parentheses; the REMD results at T = 300 K are in italics, and NA stands for not available. [b]From MD, reported by Foloppe et al.[66] using the CHARMM27 nucleic acid force field.[68] [c]Four state model. [d]Two state model. [e]From MD, reported by Lahiri et al.[28] using the CHARMM27 nucleic acid force field.[68] [f]MD in explicit solvent. [g]REMD in explicit solvent. [h]REMD in implicit solvent. [i]From MD, reported by Yildirim et al.[36] [j]NMR data reported by Plavec et al.[69] obtained at 278 K in aqueous solution. [k]NMR data reported by Dalluge et al.,[70] for Up and Dp at 25 °C. [l]Calculated from ΔG according to the equation $\%S(T) = 100\,[\exp(-\Delta G/RT)]/[\exp(-\Delta G/RT) + 1]$.[54] [m]Calculated from coupling constants ($J_{1'2'}/J_{3'4'}$) by formulas $\%S = 100[J_{1'2'}/(J_{1'2'} + J_{3'4'})]$, $\%N = 100[J_{3'4'}/(J_{1'2'} + J_{3'4'})]$ from the NMR experimental data.[49,71−73] [n]NMR data reported by Yildirim et al.,[36] values are for 30 °C. [o]From NMR data reported by Okamoto et al.[74] [p]Calculated from ΔH = 0.43 kcal·mol^{-1} and ΔS = 1.03 eu[54] at 300 K.

as described earlier for the production run in MD. The average acceptance ratio for exchange was about 70%.

Data Analysis. The averages and standard deviations for the conformational parameters were calculated from the results obtained from three separate 200 ns MD simulations for each nucleoside for each force field.

Conformational Analyses. We followed the same convention for atom names and dihedral angle nomenclature as in Saenger.[63] The magnitude of pseudorotation angle (P) was calculated according to Altona and Sundaralingam.[64] The pseudorotation space was divided into NORTH ($270° \le P < 90°$) and SOUTH ($90° \le P < 270°$) partitions to facilitate the comparison with NMR results.

The ANTI and SYN conformations of the glycosidic torsion angle (χ) measured with respect to O4′−C1′−N1−C2 were defined as the ranges 170°−300° and 30°−90°, respectively. In the case of PSU the torsion angle around O4′−C1′−C5−C4 was considered for the same.

The ranges 60° ± 30°, −60° ± 30°, and 180° ± 30° were taken to define the g^+, g^-, and trans conformations of the γ torsion angle measured with respect to O5′−C5′−C4′−C3′. We referred to values outside these ranges as other.

Hydrogen bond formations were considered between **1**. O3′−HO3′ and O2′, **2**. O2′−HO2′ and O3′ of the sugar, and **3**. C5′−OH and O2 (for U, DHU, 4SU, OAU)/S2 (for 2SU)/O4 (for PSU), **4**. C2′−OH and O2 (for U, DHU, 4SU, OAU)/S2 (for 2SU)/O4 (for PSU), **5**. C3′−H and O2 (for U, DHU, 4SU, OAU)/S2 (for 2SU)/O4 (for PSU), **6**. C2′−H and O2 (for U, DHU, 4SU, OAU)/S2 (for 2SU)/O4 (for PSU), and **7**. O5′ and C6−H6 of the base if (i) the donor−acceptor distance was ≤3.5 Å and (ii) the donor−hydrogen−acceptor angle was ≥120.0°.

The number of transitions per nanosecond for each residue between the two stable conformations in the pseudorotation space was calculated from MD trajectories considering the number of times the NORTH and SOUTH conformers left the ranges ($270° \le P < 90°$) and ($90° \le P < 270°$) respectively in a two state model.

The direct transitions from ANTI (170°−300°) to SYN (30°−90°) as well as the transitions through the intermediate regions (90°−170°, 300°−360°, or 0°−30°) were taken into account to calculate the SYN/ANTI transition rates per nanosecond.

RESULTS AND DISCUSSION

Theoretical study of tRNA using computational tools such as molecular mechanics (MM) and molecular dynamics (MD) techniques is dependent on the availability of good quality empirical force fields. Although force field parameters for the standard nucleic acid bases, nucleosides, or nucleotides were generally available for quite some time, attempts to systematically develop force fields for the modified nucleosides and nucleotides are relatively recent.[30] Remarkably, there is currently a great deal of activity where the force field parameters for the standard nucleic acid components are being critically re-examined, and various prescriptions for obtaining better agreement with experimentally observed conformational characteristics and thermodynamic properties are proposed.[33−41,65−67] In particular, the AMBER parameters[31] for the glycosidic and other torsional angles are under intensive scrutiny,[33−41,66] whereas for the CHARMM[68] force field only two torsion angle modifications have been introduced, relating to the DNA BI/BII substate equilibrium[67] and a modification of the 2′-hydroxyl torsion,[65] respectively.

In this work, along with validating the Aduri et al.[30] parameters for the AMBER FF99 force field on our test set of uridine modifications, we also examined if these recent revisions of the χ torsion angle[36,39,40] and α/γ representations[33] for regular nucleic acid residues improve force field performance for modified uridine derivatives. Only the revised χ and γ parameters are applicable for mononucleosides. We investigated the distribution of pseudorotation angle as a measure of the conformational characteristics of ribose sugar and two major torsional degrees of freedom, namely, the glycosidic torsion angle χ and the γ torsion angle that play an important

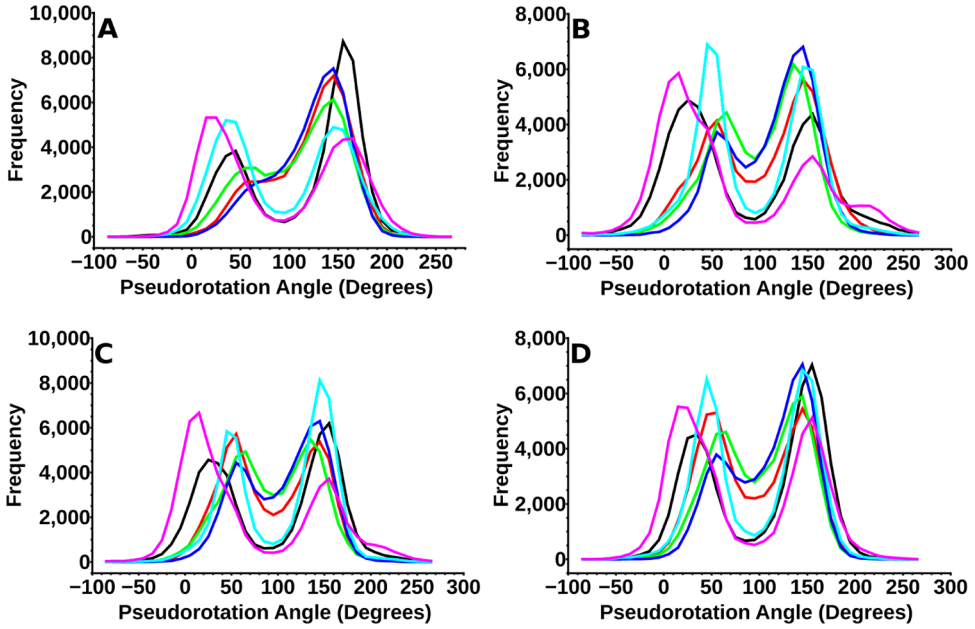

Figure 2. Population distributions (frequency vs pseudorotation angle) using total 600 ns combined MD simulations from three individual 200 ns simulations at 300 K for the nucleosides U (black), DHU (red), 2SU (green), 4SU (blue), PSU (cyan), and OAU (magenta) with A. FF99, B. FF99χ_YIL, C. FF99TOR, and D. FF10 force fields. The scale for pseudorotation angle (P) along the *X*-axis is converted to −90° to 270° to better delineate the NORTH (270° $\leq P <$ 90°) and SOUTH (90° $\leq P <$ 270°) regions.

role in maintaining the overall structural preference of nucleic acid residues and compared our results with experimental observations wherever available.

Pseudorotation Angle (*P*). The distribution of the pseudorotation angle of U averaged from three separate 200 ns MD simulation with the AMBER FF99 force field appeared to have a smaller population of the NORTH conformation in comparison to the NMR results (Table 2). Our results also agree with the conformational distribution of U reported by Yildirim et al.[36] for the FF99 force field[31] (Table 2 and Figure 2A). To check whether this discrepancy is due to convergence issues we have also included the results of 16 ns REMD simulations. Both the MD and REMD results showed noticeable deviation from NMR data (Table 2). The MD and REMD simulations of U with the FF99χ_YIL force field[36] reproduced the NMR results significantly better than the FF99 force field (Table 2, Figure 2A, Figure 2B and Figure S1A, Figure S1B, Supporting Information). For both FF99TOR[40] and FF10[39] force fields, the predicted distribution for U also showed an increased population of the NORTH conformers compared to the FF99 force field (Table 2, Figure 2 and Figure S1, Supporting Information).

Dihydrouridine was found to have a large preference for adopting the SOUTH conformation with the FF99 force field, whereas for both the FF99TOR and FF10 force fields there was a noticeable decrease in the equilibrium population of the SOUTH conformation and the equilibrium shifted toward an almost equal distribution of SOUTH and NORTH forms (Table 2, Figure 2A, Figure 2C, and Figure 2D). The best agreement with experimental sugar pucker distribution was obtained for the FF99χ_YIL force field (Table 2). The observations for DHU using MD and REMD approaches were similar for all the force fields.

NMR studies of 2SU showed that the 2-thio modification of U substantially stabilized the NORTH sugar conformation (>70%) not only at the nucleoside level but also pushed pseudorotation equilibrium of neighboring U residues toward NORTH in oligonucleotides.[54,75] The NMR data showed that the population of the NORTH conformation of 4SU was similar to that of U.[50] The FF99 force field and all other revisions of the FF99 force field considered here failed to reproduce the NMR data for 2SU and 4SU (Table 2). However, both MD and REMD simulations with the revised force fields showed a noticeable shift toward the NORTH form (Table 2, Figure 2 and Figure S1, Supporting Information).

The MD and REMD results with the FF99, FF99χ_YIL, and FF10 force fields showed almost no difference in the population of NORTH and SOUTH conformations and were very much consistent with NMR results for PSU[73,74] (Table 2, Figure 2A, Figure 2B, Figure 2D and Figure S1A, Figure S1B, Figure S1D, Supporting Information). However, simulations with the FF99TOR force field showed a slight shift toward the SOUTH conformation (Table 2).

In the case of OAU, all the revised force fields showed a preference for the NORTH form in agreement with NMR data (Figure 2).

In general, the pucker distributions of the standard nucleoside U as well as the modified nucleosides DHU, 2SU, and 4SU from both MD and REMD simulations seemed to prefer the SOUTH conformation with the FF99 force field, whereas PSU and OAU showed approximately equal distribution of SOUTH and NORTH forms (Table 2).

Although the FF99χ_YIL force field was parametrized for standard nucleosides, we found it to provide an equilibrium distribution of pseudorotation angles close to experimental observations for U, DHU, PSU, and OAU. For 2SU and 4SU, it shifted the pucker distribution toward the right direction compared to the FF99 force field.

In the case of the FF99TOR force field the average fraction of the NORTH conformation for U was less in comparison to the results obtained with the FF99χ_YIL force field (Table 2). The introduction of the revised γ parameter appears to result in

Table 3. NORTH/SOUTH Transition Rates[a] Calculated from MD Simulations[b]

	U	DHU	2SU	4SU	PSU	OAU
FF99	17.3(0.6)	33.3(0.6)	38.7(0.6)	32.0(0.0)	28.0(0.0)	20.0(0.0)
FF99χ_YIL	17.0(0.0)	35.3(0.6)	40.0(0.0)	35.3(0.6)	26.0(0.0)	17.0(1.0)
FF99TOR	17.0(0.0)	49.6(0.6)	41.6(0.6)	39.6(0.6)	26.3(0.6)	16.0(1.0)
FF10	17.6(0.6)	40.0(0.0)	41.3(2.1)	38.0(0.0)	28.3(0.6)	18.6(1.2)

[a]Transition rates (ns^{-1}) represent the number of times the NORTH and SOUTH conformers left the ranges ($270° \leq P < 90°$) and ($90° \leq P < 270°$) respectively in a two state model per nanosecond. [b]The values reported are the averages calculated from three independent 200 ns MD simulations and standard deviations are in parentheses.

Table 4. Percent (%) of Base Orientations Predicted by Various Force Fields Using Both the MD and REMD Simulations and Determined Experimentally by NMR[a]

		U	DHU	2SU	4SU	PSU	OAU
FF99	ANTI	23.0(3.6)	80.0(9.0)	94.6(1.5)	94.0(5.3)	89.3(2.1)	98.3(2.9)
		23	*82*	*94*	*95*	*92*	*98*
	SYN	66.6(3.2)	18.6(8.5)	3.3(1.5)	5.6(4.9)	9.3(1.5)	1.7(2.9)
		66	*15*	*4*	*5*	*7*	*2*
	OTHERS	10.3(0.6)	1.3(0.6)	2.0(0.0)	0.3(0.6)	1.3(0.6)	0.0(0.0)
		11	*2*	*2*	*0*	*1*	*0*
FF99χ_YIL	ANTI	83.7(2.1)	62.7(9.3)	56.7(3.2)	62.0(2.6)	18.0(1.0)	79.3(15.5)
		82	*63*	*70*	*67*	*23*	*81*
	SYN	14.3(2.1)	36.3(9.3)	36.3(3.2)	36.3(2.9)	79.0(1.0)	18.7(15.5
		15	*33*	*23*	*31*	*73*	*17*
	OTHERS	2.0(0.0)	1.0(0.0)	7.0(0.0)	1.7(0.6)	3.0(0.0)	2.0(0.0)
		2	*1*	*7*	*2*	*4*	*2*
FF99TOR	ANTI	71.0(4.4)	50.7(4.7)	60.3(2.3)	59.7(6.1)	15.7(1.5)	78.3(8.5)
		71	*68*	*64*	*61*	*13*	*64*
	SYN	27.3(4.0)	48.3(4.7)	32.7(2.3)	38.3(6.1)	81.6(2.1)	20.0(8.0)
		27	*31*	*29*	*37*	*84*	*35*
	OTHERS	1.7(0.6)	1.0(0.0)	7.0(0.0)	2.0(0.0)	2.7(0.6)	1.7(0.6)
		2	*1*	*7*	*2*	*3*	*1*
FF10	ANTI	84.3(9.6)	65.7(10.7)	74.3(16.9)	76.3(4.5)	32.7(2.3)	73.7(13.8)
		84	*69*	*78*	*78*	*32*	*64*
	SYN	14.7(9.6)	34.0(10.8)	21.7(15.9)	22.3(4.5)	63.7(2.9)	25.3(13.8)
		15	*30*	*19*	*21*	*65*	*35*
	OTHERS	1.0(0.0)	1.0(0.0)	4.0(1.0)	1.0(0.0)	3.7(0.6)	1.0(0.0)
		1	*1*	*3*	*1*	*3*	*1*
CHARMM27[b]	ANTI	98.8	NA	NA	NA	NA	NA
FF99[c]	ANTI	28	NA	NA	NA	NA	NA
FF99χ_YIL[c]	ANTI	83	NA	NA	NA	NA	NA
NMR	ANTI	93[d]	ANTI[e]	ANTI[f]	ANTI[g]	SYN[h]	NA

[a]The values reported are the averages calculated from of three independent 200 ns MD simulations, and standard deviations are in parentheses; REMD results at T = 300 K are in italics, and NA stands for not available. [b]From MD, reported by Foloppe et al.[66] using the CHARMM27 nucleic acid force field.[68] [c]From MD, reported by Yildirim et al.[36] [d]From NMR, reported by Yildirim et al.[36] [e]From NMR, reported by Deslauriers et al.[71] [f]From NMR, reported by Sierzputowska-Gracz et al.[72] [g]From NMR, reported by Hruska et al.[49] [h]From NMR, reported by Neumann et al.[46]

a shift of the NORTH/SOUTH equilibrium toward the NORTH for all the modified nucleosides except PSU.

For the FF10 force field, the pseudorotation equilibrium for U was shifted toward SOUTH in comparison to the FF99χ_YIL and FF99TOR force fields (Table 2, Figure 2B, Figure 2C, and Figure 2D). The simulated pseudorotation equilibria for PSU and OAU were in good agreement with NMR data (Table 2).

We also calculated the number of transitions between NORTH and SOUTH conformations per nanosecond from the MD trajectories to understand the extent of the conformational flexibility/rigidity of the nucleosides. We found that for each nucleoside the average transition rates were comparable for all the force fields (Table 3) except for DHU. The predicted average transition rate with the FF99TOR force field for DHU was found to be higher than that of the other force fields. In general all the modifications except OAU showed an increased transition rate in comparison to U. We found that the transition rates for 2SU for all the force fields were considerably high and similar to DHU (Table 3, Figure S4, Figure S5, Figure S6, and Figure S7, Supporting Information). This was surprising considering that 2SU is generally thought to promote conformational rigidity in contrast to DHU which is supposed to induce conformational flexibility.[70,75,76]

Glycosidic Torsion Angle (χ). It was previously suggested that the SYN conformation is particularly unfavorable in pyrimidines.[77,78] NMR studies of U, DHU, 2SU, and 4SU showed a preference for the ANTI conformation (Table 4).[36,49,71,72] The ANTI conformation was reported to be preferred for 2-thiopyrimidines also.[79] An optical rotatory dispersion (ORD) study[80] of U and X-ray crystallography[81] supports NMR results.[36] From NMR, the ANTI conformation

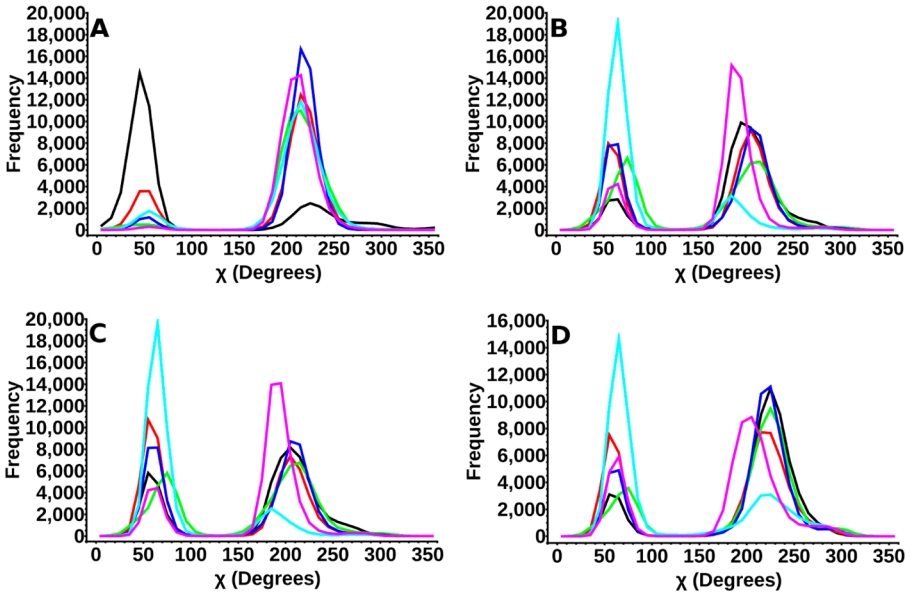

Figure 3. Population distributions (frequency vs χ torsion) using total 600 ns combined MD simulations from three individual 200 ns simulations at 300 K for the nucleosides U (black), DHU (red), 2SU (green), 4SU (blue), PSU (cyan), and OAU (magenta) with A. FF99, B. FF99χ_YIL, C. FF99TOR, and D. FF10 force fields.

Table 5. SYN/ANTI Transition Rates[a] Calculated from MD Simulations[b]

	U	DHU	2SU	4SU	PSU	OAU
FF99	0.44(0.02)	0.06(0.02)	0.07(0.02)	0.02(0.01)	0.15(0.01)	0.00(0.01)
FF99χ_YIL	0.14(0.05)	0.08(0.01)	0.08(0.02)	0.22(0.02)	0.31(0.02)	0.03(0.02)
FF99TOR	0.18(0.02)	0.07(0.01)	0.08(0.01)	0.21(0.04)	0.29(0.04)	0.03(0.01)
FF10	0.05(0.02)	0.05(0.01)	0.03(0.01)	0.10(0.03)	0.48(0.02)	0.03(0.01)

[a]Transition (ns^{-1}) represents the direct transitions from ANTI (170°−300°) to SYN (30°−90°) as well as the transitions through the intermediate regions (90°−170°, 300°−360°, or 0°−30°). [b]The values reported are the averages calculated from three independent 200 ns MD simulations, and the standard deviations are in parentheses.

was indicated for 4-thiouridine-5′-phosphate in single-stranded oligo- and polynucleotides, whereas it was assumed from the ORD curve of the copolymer consisting of uridine-5′-phosphate and 4-thiouridine-5′-phosphate that 4-thiouridine-5′-phosphate in double-helical polynucleotides preferred the SYN conformation.[82] An X-ray crystallographic study of 4SU reported a NORTH/SYN conformation[50] although NMR results suggested the ANTI conformation in aqueous solution.[49] Conformational studies of PSU as a free nucleoside and as a part of yeast $tRNA^{Phe}$ and its derivative pseudouridine 3′-monophosphate indicated a preference for the SYN conformation.[46,83] In the crystal structure of the methyl ester of OAU, the glycosidic torsion angle was observed in the ANTI conformation.[55]

Uridine preferentially adopted the SYN conformation with the FF99 force field, whereas for all the modified nucleosides, the SYN/ANTI equilibrium was shifted toward the ANTI conformation (Table 4, Figure 3A). The REMD results for the FF99 force field were observed to be in close correspondence with MD results for all the nucleosides under study (Table 4 and Figure S2A, Supporting Information).

The glycosidic torsional equilibrium for U preferentially adopted the ANTI conformation with the FF99χ_YIL force field, whereas for all the modified uridine derivatives the ANTI conformation remained the preferred one but their population was less compared to the FF99 force field (Table 4, Figures 3A and 3B). Surprisingly, for PSU the SYN/ANTI equilibrium was found to be shifted toward SYN much more for all the revised force fields in comparison to the FF99 force field (Table 4, Figure 3).

The distribution of glycosidic torsion for U obtained from the FF99TOR force field was not significantly different from the FF99χ_YIL results (Table 4, Figure 3B, Figure 3C and Figure S2B and Figure S2C, Supporting Information). In the case of the FF10 force field, a strong preference for the ANTI orientation was observed for the residues U, DHU, 2SU, 4SU, and OAU from our simulations which were in general agreement with experimental observations (Table 4, Figure 3D and Figure S2D, Supporting Information). In the case of PSU, SYN was found to be preferred.

Overall, it was found that the revised γ parameter of Perez et al.[33] did not significantly affect the SYN/ANTI equilibrium for the studied nucleosides. All the revised force fields provided a better equilibrium description than the FF99 force field.

The direct transitions from ANTI (170°−300°) to SYN (30°−90°) along with the transitions through the intermediate regions were summarized in Table 5. Overall, the revised force fields showed a large transition rate for 4SU and PSU (except FF10 for 4SU), whereas DHU along with OAU showed a much reduced transition rate (Table 5, Figure S8, Figure S9, Figure S10, and Figure S11, Supporting Information).

γ Torsion Angle. We have calculated the population of the g+ conformation from $J_{4'5'}$ and $J_{4'5''}$ coupling constants[75,84,85] of U, DHU, 2SU, 4SU, and PSU.[49,71−73] We found that the g+ population was >90% only for 2SU, and for the others, it was around 60% (Table 6).

dx.doi.org/10.1021/ci400582a | J. Chem. Inf. Model. 2014, 54, 1129−1142

Table 6. Percent (%) of the γ Population Predicted by Various Force Fields Using Both the MD and REMD Simulations[a]

		U	DHU	2SU	4SU	PSU	OAU
FF99	g^+	58.7(0.6)	33.7(3.1)	34.7(1.5)	35.7(2.1)	47.3(2.9)	57.0(1.7)
		68	*37*	*32*	*35*	*52*	*64*
	g^-	0.0(0.0)	27.0(2.0)	23.7(2.1)	25.0(1.0)	1.0(0.0)	0.6(0.6)
		0	*24*	*25*	*25*	*1*	*0*
	trans	38.3(0.6)	37.7(1.5)	40.3(0.6)	37.7(1.2)	47.7(2.9)	38.3(2.1)
		30	*38*	*42*	*38*	*43*	*32*
	others	3.0(0.0)	1.7(0.6)	1.3(0.6)	1.7(0.6)	4.4(0.0)	4.0(0.0)
		2	*1*	*1*	*2*	*4*	*4*
FF99χ_YIL	g^+	45.0(3.6)	30.3(2.1)	35.7(3.2)	32.0(2.6)	53.0(1.0)	52.3(1.2)
		40	*27*	*35*	*41*	*49*	*50*
	g^-	0.0(0.0)	26.7(2.5)	24.0(1.7)	26.3(1.5)	1.0(0.0)	1.0(0.0)
		0	*31*	*24*	*27*	*1*	*1*
	trans	51.3(3.1)	41.7(1.2)	38.7(2.5)	40.0(1.7)	43.0(1.0)	43.7(1.2)
		56	*41*	*39*	*31*	*46*	*45*
	others	3.7(0.6)	1.3(0.6)	1.7(0.6)	1.7(0.6)	3.0(0.0)	3.0(0.0)
		4	*1*	*2*	*1*	*4*	*4*
FF99TOR	g^+	91.0(1.0)	89.3(2.9)	89.7(3.2)	92.3(2.9)	89.0(1.7)	90.3(1.2)
		92	*89*	*91*	*91*	*91*	*92*
	g^-	4.3(0.6)	8.0(4.4)	8.0(1.7)	6.0(1.7)	7.7(0.6)	7.0(1.0)
		3	*7*	*8*	*6*	*7*	*6*
	trans	4.3(1.2)	2.3(1.2)	1.7(1.2)	3.0(1.0)	3.0(1.0)	2.3(0.6)
		4	*4*	*3*	*2*	*2*	*1*
	others	0.0(0.0)	0.0(0.0)	0.0(0.0)	0.0(0.0)	0.0(0.0)	0.0(0.0)
		1	*0*	*0*	*0*	*0*	*1*
FF10	g^+	92.7(1.5)	89.3(3.8)	91.0(1.0)	90.7(1.2)	86.3(1.5)	88.7(3.1)
		94	*90*	*93*	*92*	*87*	*88*
	g^-	4.7(0.6)	8.3(3.2)	6.3(1.2)	7.0(1.7)	10.0(1.7)	9.0(2.6)
		3	*7*	*5*	*7*	*11*	*10*
	trans	2.3(0.6)	2.3(0.6)	2.7(0.6)	2.3(1.5)	3.3(0.6)	1.7(0.6)
		2	*3*	*2*	*1*	*2*	*2*
	others	0.0(0.0)	0.0(0.0)	0.0(0.0)	0.0(0.0)	0.0(0.0)	0.0(0.0)
		1	*0*	*0*	*0*	*0*	*0*
CHARMM27[b]	g^+	93.8	NA	NA	NA	NA	NA
NMR[C]	g^+	66, 63	53	91	64	59	NA

[a]The values reported are the averages calculated from of three independent 200 ns MD simulations, and the standard deviations are in parentheses; REMD results at T = 300 K are in italics, and NA stands for not available. [b]From MD, reported by Foloppe et al.[66] using the CHARMM27 nucleic acid force field.[68] [C]Calculated from coupling constants ($J_{4'5'}/J_{4'5''}$) by formulas % $\gamma = [((13.75 - J_{4'5'} - J_{4'5''})/10.05) \times 100]$[75,84,85] from the NMR experimental data.[49,71−73]

The X-ray crystallographic study of two molecular conformations present in the asymmetric unit of crystals of DHU showed the g^- orientation of the γ torsion angle in one conformation, whereas in the other conformation there was a mixture of 88% trans and 12% g^+ orientations.[86] The NMR study of DHU showed a distinct preference for the g^+ conformation along with the presence of g^- and trans conformations.[71] An NMR study of 2-thiopyrimidines also suggested a preference for the g^+ conformation.[79] A comparative NMR study of U and β-PSU showed a similar conformational preference of the γ torsion angle for the g^+ conformation.[46] The X-ray crystallographic study of the methyl ester of OAU found the γ torsion angle to be within the range for the g^+ conformation.[55]

In our simulations, similar results were observed for the distribution of the γ torsion angle for the FF99 and FF99χ_YIL force fields. The γ torsion angles for U, PSU, and OAU were preferentially distributed between g^+ and trans conformations with negligible g^- populations (Table 6, Figure 4A, Figure 4B and Figure S3A and S3B, Supporting Information).

However, for DHU, 2SU, and 4SU, the g^- form was significantly populated along with g^+ and trans conformations. The FF99TOR and FF10 force fields with the revised γ parameter showed increased g^+ populations (Table 6). Perez et al.[33] carried out the refinement of the α/γ torsional terms to overcome the problem of overpopulation of the trans conformation observed with the FF99 force field. Accordingly, our observation of a very high preference for the g^+ conformation and a negligible amount of g^- and trans populations with both the FF99TOR and FF10 force fields for all the regular and modified nucleosides was according to expectations (Table 6, Figure 4C, Figure 4D and Figure S3C, S3D, Supporting Information).

The frequency of transition between g^+, g^-, and trans conformations was found to be appreciably lower for the FF99TOR and FF10 force fields compared to the FF99 and FF99χ_YIL force fields (Figure S12, Figure S13, Figure S14, and Figure S15, Supporting Information).

Correlation of the Glycosidic Torsion Angle (χ) with the Pseudorotation Equilibrium. We prepared a full set of correlation maps in the form of 2D scattergrams of

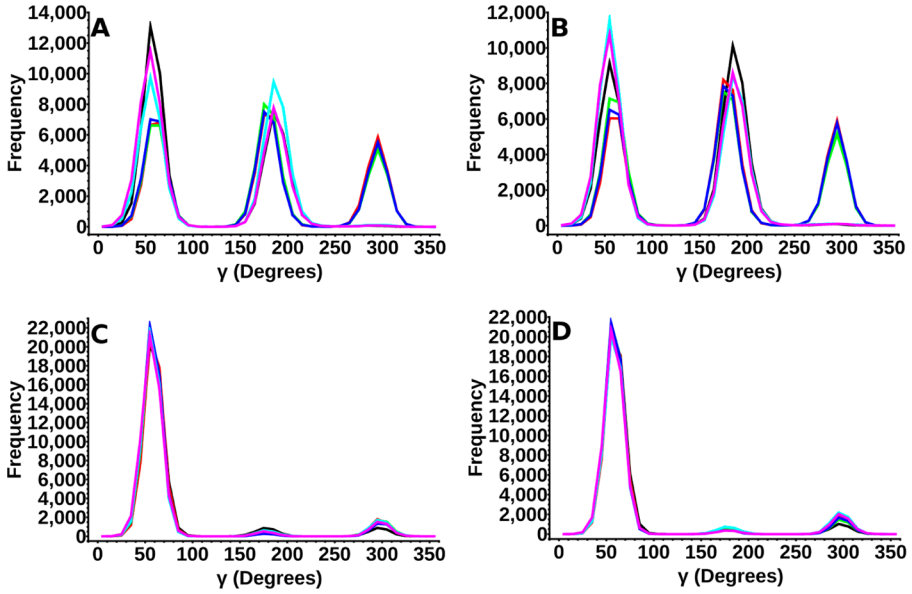

Figure 4. Population distributions (frequency vs γ torsion) using total 600 ns combined MD simulations of three individual 200 ns simulations at 300 K for the nucleosides U (black), DHU (red), 2SU (green), 4SU (blue), PSU (cyan), and OAU (magenta) with A. FF99, B. FF99χ_YIL, C. FF99TOR, and D. FF10 force fields.

pseudorotation angles (P) versus glycosidic torsion angles (χ) for the nucleosides under study (Figure S16–Figure S21, Supporting Information).

A thorough analysis of X-ray crystallographic results suggested that, in purines, the SYN conformation has a significant correlation with SOUTH sugar pucker[78,87,88] and the NORTH form with ANTI.[89] In pyrimidines, it is relatively rare to find the SYN orientation of the base moiety. It was observed from the NMR study that pyrimidines were conformationally more restricted than purines around the glycosidic bond and the ANTI conformation dominates over SYN.[90] Modified pyrimidines in which the C6 has been substituted with bulky groups may shift the SYN/ANTI equilibrium toward SYN.[91] NMR and CD spectroscopic data also support crystallographic data and indicate rapid interchange between the SYN and ANTI conformation in solution.[90] In particular, for the set of nucleosides chosen in this work, experiments indicate preferences for NORTH/ANTI for U, 2SU, 4SU, and OAU,[36,49,54,55,69,70,72] SOUTH/ANTI for DHU,[70,71] and almost equal NORTH/SOUTH and SYN for PSU,[46,73,74] respectively.

From the present set of simulations, the major observations were as follows:

1. The 2D correlation map for U with the FF99 force field indicated a clear preference for the SOUTH/SYN conformation (Figure S16, Supporting Information). Both FF99χ_YIL and FF99TOR force fields favored NORTH/ANTI conformations, whereas the FF10 force field showed a marked preference for the SOUTH/ANTI conformation (Figure S16, Supporting Information).

2. For DHU, the FF99 and FF99χ_YIL force fields clearly favored the SOUTH/ANTI conformation (Figure S17, Supporting Information).

3. For 2SU, FF99, FF99χ_YIL, and FF10 force fields shifted the overall equilibrium toward SOUTH/ANTI, and the equilibrium population was preferentially ANTI with almost equal NORTH and SOUTH conformations for the FF99TOR force field (Figure S18, Supporting Information).

4. The FF99 and all the revised force fields favored the SOUTH/ANTI conformation for 4SU (Figure S19, Supporting Information).

5. Remarkably for PSU, the FF99 force field showed an almost equal distribution of NORTH/ANTI and SOUTH/ANTI conformations and a negligible population of the SYN orientation. NORTH/SYN and SOUTH/SYN conformations were found to be almost equally populated for all the revised force fields (Figure S20, Supporting Information).

6. The conformational distribution for OAU with the FF99 force field showed an almost complete absence of SYN conformations, and the population of the NORTH/ANTI conformation seemed to be slightly larger than that of the SOUTH/ANTI conformation. All the revised FF99 force fields also seemed to favor the NORTH/ANTI conformation for OAU (Figure S21, Supporting Information).

From the above observations it appears that except for DHU and OAU, the distributions for the other nucleosides with the FF99 force field did not agree well with experimentally observed results. On the other hand, the FF99χ_YIL force field was found to better reproduce the pseudorotation equilibrium for U, DHU, PSU, and OAU and the χ torsional distributions for all the nucleosides. The FF99TOR force field did not show any significant improvement over the FF99χ_YIL force field. The results obtained with the FF10 force field were close to the experimental observations only for PSU and OAU.

Hydrogen Bonding Characteristics. We investigated the extent of hydrogen bond formation within the sugar moiety and also between sugar and base atoms for all the force fields. Here we considered the extent of formation of five types of hydrogen bonding interactions between sugar and base when χ was in either ANTI or SYN conformations. We also studied the extent of formation of two types of hydrogen bonding interactions within the sugar moiety that were suggested to stabilize the NORTH and SOUTH conformations from a quantum chemical study.[92]

Among the interactions that were supposed to stabilize the SYN conformation, the O5′–H···O2 (in U, DHU, 4SU,

dx.doi.org/10.1021/ci400582a | J. Chem. Inf. Model. 2014, 54, 1129–1142

OAU)/O5′−H···S2 (in 2SU)/O5′−H···O4 (in PSU) interactions were observed to form in a significant proportion of the simulation period. In X-ray crystallographic study of SYN nucleosides, this interaction in pyrimidines was thought to stabilize the SYN orientation of base with respect to the sugar moiety[93] although there are exceptions indicating that favorable orientation of O5′ and O2 did not guarantee the formation of this hydrogen bond.[50,88] Our results indicated that these hydrogen bonds were formed in a significant amount of the SYN population for all the nucleosides with all the force fields (except in OAU for the FF99 force field) (Table S1, Supporting Information). For the FF99TOR and FF10 force fields, increased percentages of the SYN population forming this type of hydrogen bond compared to the other two force fields were observed. It indicated a probable role of the revised γ torsion angle parameter in favoring this hydrogen bond formation.

The other types of SYN stabilizing hydrogen bonding interactions studied were C3′−H3′···O2 (in U, DHU, 4SU, OAU)/S2 (in 2SU)/O4 (in PSU) and C2′−H2′···O2 (in U, DHU, 4SU, OAU)/S2 (in 2SU)/O4 (in PSU) interactions. In our calculations we found only a small population of SYN conformations favoring these hydrogen bonds (Table S2, Supporting Information).

Among interactions that were thought to stabilize the ANTI conformation, the O2′−H···O2 (in U, DHU, 4SU, OAU)/O2′−H···S2 (in 2SU)/O2′−H···O4 (in PSU) interactions were found to be formed only for a small population of ANTI conformations for all the nucleosides for all of the force fields (Table S3, Supporting Information).

Quantum chemical calculations (CNDO/2) considering the forces and energies involved in base−C−H···O5′ interactions concluded that base−C−H···O5′ hydrogen bonding may influence the stabilization of the g^+, ANTI conformation of uridine, thymidine, and 5-fluorouridine.[94] These calculations were in accordance with X-ray crystallographic observation which showed that in pyrimidine the C6···O5′ distance is significantly less than the sum of van der Waals radii of O and H atoms.[85] Electron withdrawing groups attached to pyrimidine C6 can also facilitate this hydrogen bonding and may stabilize the ANTI, g^+ conformation.[95] The C6−H6···O5′ hydrogen bond, which was expected to stabilize the ANTI conformation, was found to form for a significant amount of the ANTI population only for OAU with respect to other nucleosides for all the force fields under study (Table S4, Supporting Information).

Hydrogen bonding interactions within the sugar moiety that are thought to stabilize NORTH and SOUTH conformations, namely the O2′−HO2′···O3′ and O3′−HO3′···O2′ interactions respectively, were observed in quantum chemical studies of the natural nucleosides 2′-deoxyuridine and uridine.[92] As the NORTH and SOUTH sugar puckering were reported to be correlated with ANTI and SYN orientations, respectively,[96] these two hydrogen bonding interactions may also be correlated with the distribution of ANTI and SYN conformers. In our simulations these two hydrogen bonds were found to form almost similarly in a small amount for ANTI and SYN populations, except for uridine which showed a slightly higher fraction of ANTI and SYN populations forming the O3′−HO3′···O2′ than that of the O2′−HO2′···O3′ bond (Table S5, Supporting Information).

CONCLUSIONS

In this work we have carried out MD and REMD simulations of five modified uridines (DHU, 2SU, 4SU, PSU, and OAU) with the aim of validating the parameters developed by Aduri et al.[30] for modified RNAs for the AMBER FF99 force field. We also combined this set of parameters with three recently proposed revisions of the FF99 force field for regular nucleic acid residues, namely FF99χ_YIL with revised χ parameters, and FF99TOR and FF10 with different combinations of revised χ and γ parameters to examine its transferability. Additionally, we carried out MD and REMD simulations of uridine for all the four force fields as controls. The choice of such small systems for parameter validation reduced the sampling problem and also allowed for comparison with NMR results on equilibrium distribution of conformational degrees of freedom.

Our calculations showed that for the FF99 force field, the distribution for the pseudorotation angle and the glycosidic torsion angle were consistent with experimental results only for DHU and OAU. For 2SU and 4SU, the prediction of sugar pucker distribution was wrong, while for PSU the preferred distribution of the glycosidic torsion was predicted incorrectly.

The combination of the Aduri et al.[30] parameters with the FF99χ_YIL force field led to noticeable improvements in that the preference for the ANTI or the SYN conformation was consistent with experimental observations for all of the five modified uridines. Consequently, this combination simulated the behavior of the pucker and glycosidic torsion accurately for DHU, PSU, and OAU. However, it was still insufficient for predicting correctly the conformational preferences of 2SU and 4SU.

The combination of the Aduri et al.[30] parameter sets with the FF99TOR and FF10 force fields did not improve significantly the correspondence between the simulated conformational distributions and experimental observations further. The results for PSU and OAU were similar as in the case of the FF99χ_YIL force field. Considering the γ distribution, the noticeable difference observed as a whole with the FF99TOR and FF10 force fields was the shifting of the equilibrium population of g^+ to a very high value and an almost negligible occurrence of g^- and trans populations with respect to the FF99 and FF99χ_YIL force fields. This observation was in accordance with the increasing population of the SYN conformation favoring the O5′−H···O2 (for DHU, 4SU, OAU)/O5′−H···S2 (for 2SU)/O5′−H···O4 (for PSU) hydrogen bond.

The above observations necessitate a thorough revision of the parameter set for AMBER developed by Aduri et al.[30] for modified RNAs. It also shows, as perhaps expected, that the recent revisions of the AMBER force fields have been constructed in a way which made the Aduri et al.[30] parameters for the modifications not transferable except for particular cases. Seemingly, the only way of obtaining accurate parameters for nucleic acid modifications would be by reoptimizing the torsion angles for each individual modified residue and validating with larger RNA structures. We are currently working on that problem.

ASSOCIATED CONTENT

Supporting Information

Figure S1, population distributions (frequency vs pseudorotation angle) from 16 ns REMD simulations at 300 K of the nucleosides U, DHU, 2SU, 4SU, PSU, and OAU with FF99, FF99χ_YIL, FF99TOR, and FF10 force fields; Figure S2,

population distributions (frequency vs χ torsion) from 16 ns REMD simulations at 300 K of the nucleosides U, DHU, 2SU, 4SU, PSU, and OAU with FF99, FF99χ_YIL, FF99TOR, and FF10 force fields; Figure S3, population distributions (frequency vs γ torsion) from 16 ns REMD simulations at 300 K of the nucleosides U, DHU, 2SU, 4SU, PSU, and OAU with FF99, FF99χ_YIL, FF99TOR, and FF10 force fields; Figure S4, fluctuation time series of pseudorotation angle (P) of nucleosides with FF99 force field; Figure S5, fluctuation time series of pseudorotation angle (P) of nucleosides with FF99χ_YIL force field; Figure S6, fluctuation time series of pseudorotation angle (P) of nucleosides with FF99TOR force field; Figure S7, fluctuation time series of pseudorotation angle (P) of nucleosides with FF10 force field; Figure S8, fluctuation time series of glycosidic torsion angle (χ) of nucleosides with FF99 force field; Figure S9, fluctuation time series of glycosidic torsion angle (χ) of nucleosides with FF99χ_YIL force field; Figure S10, fluctuation time series of glycosidic torsion angle (χ) of nucleosides with FF99TOR force field; Figure S11, fluctuation time series of glycosidic torsion angle (χ) of nucleosides with FF10 force field; Figure S12, fluctuation time series of γ torsion angle of nucleosides with FF99 force field; Figure S13, fluctuation time series of γ torsion angle of nucleosides with FF99χ_YIL force field; Figure S14, fluctuation time series of γ torsion angle of nucleosides with FF99TOR force field; Figure S15, fluctuation time series of γ torsion angle of nucleosides with FF10 force field; Figure S16: 2D scattergram for pseudorotation angle (P) versus glycosidic torsion angle (χ) for U for A. FF99, B. FF99χ_YIL, C. FF99TOR, and D. FF10 force fields; Figure S17: 2D scattergram for pseudorotation angle (P) versus glycosidic torsion angle (χ) for DHU for A. FF99, B. FF99χ_YIL, C. FF99TOR, and D. FF10 force fields; Figure S18: 2D scattergram for pseudorotation angle (P) versus glycosidic torsion angle (χ) for 2SU for A. FF99, B. FF99χ_YIL, C. FF99TOR, and D. FF10 force fields; Figure S19: 2D scattergram for pseudorotation angle (P) versus glycosidic torsion angle (χ) for 4SU for A. FF99, B. FF99χ_YIL, C. FF99TOR, and D. FF10 force fields; Figure S20: 2D scattergram for pseudorotation angle (P) versus glycosidic torsion angle (χ) for PSU for A. FF99, B. FF99χ_YIL, C. FF99TOR, and D. FF10 force fields; Figure S21: 2D scattergram for pseudorotation angle (P) versus glycosidic torsion angle (χ) for OAU for A. FF99, B. FF99χ_YIL, C. FF99TOR, and D. FF10 force fields; Table S1, percent (%) of the SYN conformation favoring the O5′−H---O2 (for U, DHU, 4SU, OAU)/S2 (for 2SU)/O4 (for PSU) hydrogen bond; Table S2, percent (%) of the SYN conformation favoring the C3′−H3′/C2′−H2′---O2 (for U, DHU, 4SU, OAU)/S2 (for 2SU)/O4 (for PSU) hydrogen bond; Table S3, percent (%) of the ANTI conformation favoring the O2′−HO2′---O2 (for U, DHU, 4SU, OAU)/S2 (for 2SU)/O4 (for PSU) hydrogen bond; Table S4, percent (%) of the ANTI conformation favoring the base−C6−H6---O5′ hydrogen bond; Table S5, percent (%) of ANTI and SYN conformations favoring the O3′−HO3′---O2′ and O3′---HO2′−O2′ hydrogen bonds, respectively. This material is available free of charge via the Internet at http://pubs.acs.org.

AUTHOR INFORMATION

Corresponding Author

*Phone: +913323508386 extn. 329. Fax: +9123519755. E-mail: lahiri.ansuman@gmail.com.

Notes

The authors declare no competing financial interest.

ACKNOWLEDGMENTS

Indrajit Deb would like to acknowledge support from the UGC RFSMS program and subsequent CSIR Senior Research Fellowship. This research work was partially supported by UGC-MAJOR project [F41-948/2012(SR)] and also by the departmental DST-FIST and UGC-DSA programs. The BIOGENE high performance computing facility at the Bioinformatics Resources and Applications Facility (BRAF) at C-DAC, Pune and the Centre for High Performance Computing for Modern Biology, Ballygunge Science College, University of Calcutta are acknowledged for providing us generous computational support. The authors wish to thank Agnieszka Mickiewicz for help with data analysis and Douglas H. Turner, Ilyas Yildirim, and particularly David Condon for their help, valuable suggestions, and discussions regarding the initial setup of the FF99χ_YIL force field.

REFERENCES

(1) Cantara, W. A.; Crain, P. F.; Rozenski, J.; McCloskey, J. A.; Harris, K. A.; Zhang, X.; Vendeix, F. A.; Fabris, D.; Agris, P. F. The RNA; Modification Database, RNAMDB: 2011 Update. *Nucleic Acids Res.* **2011**, *39*, D195−D201.

(2) Machnicka, M. A.; Milanowska, K.; Oglou, O. O.; Purta, E.; Kurkowska, M.; Olchowik, A.; Januszewski, W.; Kalinowski, S.; Dunin-Horkawicz, S.; Rother, K. M.; Helm, M.; Bujnicki, J. M.; Grosjean, H. MODOMICS: A Database of RNA Modification Pathways—2013 Update. *Nucleic Acids Res.* **2013**, *41*, D262−D267.

(3) Sprinzl, M.; Vassilenko, K. S. Compilation of tRNA Sequences and Sequences of tRNA Genes. *Nucleic Acids Res.* **2005**, *33*, D139−D140.

(4) Phizicky, E. M.; Alfonzo, J. D. Do All Modifications Benefit All tRNAs? *FEBS Lett.* **2010**, *584*, 265−271.

(5) Helm, M.; Giege, R.; Florentz, C. A Watson-Crick Base-Pair-Disrupting Methyl Group (m1A9) Is Sufficient for Cloverleaf Folding of Human Mitochondrial tRNALys. *Biochemistry* **1999**, *38*, 13338−13346.

(6) Cabello-Villegas, J.; Winkler, M. E.; Nikonowicz, E. P. Solution Conformations of Unmodified and A(37)N(6)-Dimethylallyl Modified Anticodon Stem-Loops of *Escherichia coli* tRNA(Phe). *J. Mol. Biol.* **2002**, *319*, 1015−1034.

(7) Tworowska, I.; Nikonowicz, E. P. Base Pairing within the ψ32,ψ39-Modified Anticodon Arm of *Escherichia coli* tRNAPhe. *J. Am. Chem. Soc.* **2006**, *128*, 15570−15571.

(8) Helm, M. Post-Transcriptional Nucleotide Modification and Alternative Folding of RNA. *Nucleic Acids Res.* **2006**, *34*, 721−733.

(9) Kobitski, A. Y.; Hengesbach, M.; Helm, M.; Nienhaus, G. U. Sculpting an RNA Conformational Energy Landscape by a Methyl Group Modification–a Single-Molecule FRET Study. *Angew. Chem., Int. Ed. Engl.* **2008**, *47*, 4326−4330.

(10) Motorin, Y.; Helm, M. tRNA Stabilization by Modified Nucleotides. *Biochemistry* **2010**, *49*, 4934−4944.

(11) Kobitski, A. Y.; Hengesbach, M.; Seidu-Larry, S.; Dammertz, K.; Chow, C. S.; van Aerschot, A.; Nienhaus, G. U.; Helm, M. Single-Molecule FRET Reveals a Cooperative Effect of Two Methyl Group Modifications in the Folding of Human Mitochondrial tRNA(Lys). *Chem. Biol.* **2011**, *18*, 928−936.

(12) Decatur, W. A.; Fournier, M. J. rRNA Modifications and Ribosome Function. *Trends Biochem. Sci.* **2002**, *27*, 344−351.

(13) Chow, C. S.; Lamichhane, T. N.; Mahto, S. K. Expanding the Nucleotide Repertoire of the Ribosome with Post-transcriptional Modifications. *ACS Chem. Biol.* **2007**, *2*, 610−619.

(14) El Yacoubi, B.; Bailly, M.; de Crecy-Lagard, V. Biosynthesis and Function of Posttranscriptional Modifications of Transfer RNAs. *Annu. Rev. Genet.* **2012**, *46*, 69−95.

(15) Carell, T.; Brandmayr, C.; Hienzsch, A.; Muller, M.; Pearson, D.; Reiter, V.; Thoma, I.; Thumbs, P.; Wagner, M. Structure and Function of Noncanonical Nucleobases. *Angew. Chem., Int. Ed.* **2012**, *51*, 7110−7131.
(16) Jackman, J. E.; Alfonzo, J. D. Transfer RNA Modifications: Nature's Combinatorial Chemistry Playground. *Wiley Interdiscip. Rev.: RNA* **2013**, *4*, 35−48.
(17) Mahto, S. K.; Chow, C. S. Probing the Stabilizing Effects of Modified Nucleotides in the Bacterial Decoding Region of 16S Ribosomal RNA. *Bioorg. Med. Chem.* **2013**, *21*, 2720−2726.
(18) Byrne, R. T.; Konevega, A. L.; Rodnina, M. V.; Antson, A. A. The Crystal Structure of Unmodified tRNAPhe from Escherichia Coli. *Nucleic Acids Res.* **2010**, *38*, 4154−4162.
(19) Agris, P. F. Wobble Position Modified Nucleosides Evolved To Select Transfer RNA Codon Recognition: A Modified-Wobble Hypothesis. *Biochimie* **1991**, *73*, 1345−1349.
(20) Stuart, J. W.; Koshlap, K. M.; Guenther, R.; Agris, P. F. Naturally-Occurring Modification Restricts the Anticodon Domain Conformational Space of tRNAPhe. *J. Mol. Biol.* **2003**, *334*, 901−918.
(21) Agris, P. F. Decoding the Genome: A Modified View. *Nucleic Acids Res.* **2004**, *32*, 223−238.
(22) Agris, P. F.; Vendeix, F. A. P.; Graham, W. D. tRNA's Wobble Decoding of the Genome: 40 Years of Modification. *J. Mol. Biol.* **2007**, *366*, 1−13.
(23) Agris, P. F. Bringing Order to Translation: The Contributions of Transfer RNA Anticodon-Domain Modifications. *EMBO Rep.* **2008**, *9*, 629−635.
(24) Lind, K. E.; Mohan, V.; Manoharan, M.; Ferguson, D. M. Structural Characteristics of 2′-O-(2-methoxyethyl)-Modified Nucleic Acids from Molecular Dynamics Simulations. *Nucleic Acids Res.* **1998**, *26*, 3694−3699.
(25) Auffinger, P.; Louise-May, S.; Westhof, E. Molecular Dynamics Simulations of Solvated Yeast tRNA(Asp). *Biophys. J.* **1999**, *76*, 50−74.
(26) Auffinger, P.; Westhof, E. RNA Solvation: A Molecular Dynamics Simulation Perspective. *Biopolymers* **2000**, *56*, 266−274.
(27) McCrate, N. E.; Varner, M. E.; Kim, K. I.; Nagan, M. C. Molecular Dynamics Simulations of Human tRNALys,3 UUU: The Role of Modified Bases in mRNA Recognition. *Nucleic Acids Res.* **2006**, *34*, 5361−5368.
(28) Lahiri, A.; Sarzynska, J.; Nilsson, L.; Kulinski, T. Molecular Dynamics Simulation of the Preferred Conformations of 2-thiouridine in Aqueous Solution. *Theor. Chem. Acc.* **2007**, *117*, 267−273.
(29) Eargle, J.; Black, A. A.; Sethi, A.; Trabuco, L. G.; Luthey-Schulten, Z. Dynamics of Recognition Between tRNA and Elongation Factor Tu. *J. Mol. Biol.* **2008**, *377*, 1382−1405.
(30) Aduri, R.; Psciuk, B. T.; Saro, P.; Taniga, H.; Schlegel, H. B.; SantaLucia, J., Jr. AMBER Force Field Parameters for the Naturally Occurring Modified Nucleosides in RNA. *J. Chem. Theory Comput.* **2007**, *3*, 1464−1475.
(31) Wang, J.; Cieplak, P.; Kollman, P. A. How Well Does a Restrained Electrostatic Potential (RESP) Model Perform in Calcluating Conformational Energies of Organic and Biological Molecules? *J. Comput. Chem.* **2000**, *21*, 1049−1074.
(32) Cornell, W. D.; Cieplak, P.; Bayly, C. I.; Gould, I. R.; Merz, K. M.; Ferguson, D. M., Jr.; Spellmeyer, D. C.; Fox, T.; Caldwell, J. W.; Kollman, P. A. A Second Generation Force Field for the Simulation of Proteins, Nucleic Acids, and Organic Molecules. *J. Am. Chem. Soc.* **1995**, *117*, 5179−5197.
(33) Perez, A.; Marchan, I.; Svozil, D.; Sponer, J.; Cheatham, T. E.; Laughton, C. A.; Orozco, M. Refinement of the AMBER Force Field for Nucleic Acids: Improving the Description of Alpha/Gamma Conformers. *Biophys. J.* **2007**, *92*, 3817−3829.
(34) Ode, H.; Matsuo, Y.; Neya, S.; Hoshino, T. Force Field Parameters for Rotation Around χ Torsion Axis in Nucleic Acids. *J. Comput. Chem.* **2008**, *29*, 2531−2542.
(35) Gong, Z.; Xiao, Y. RNA Stability Under Different Combinations of Amber Force Fields and Solvation Models. *J. Biomol. Struct. Dyn.* **2010**, *28*, 431−441.
(36) Yildirim, I.; Stern, H. A.; Kennedy, S. D.; Tubbs, J. D.; Turner, D. H. Reparameterization of RNAχ Torsion Parameters for the AMBER Force Field and Comparison to NMR Spectra for Cytidine and Uridine. *J. Chem. Theory Comput.* **2010**, *6*, 1520−1531.
(37) Banas, P.; Hollas, D.; Zgarbova, M.; Jurecka, P.; Orozco, M.; Cheatham, T. E., III; Sponer, J.; Otyepka, M. Performance of Molecular Mechanics Force Fields for RNA Simulations: Stability of UUCG and GNRA Hairpins. *J. Chem. Theory Comput.* **2010**, *6*, 3836−3849.
(38) Yildirim, I.; Stern, H. A.; Tubbs, J. D.; Kennedy, S. D.; Turner, D. H. Benchmarking AMBER Force Fields for RNA: Comparisons to NMR Spectra for Single-Stranded r(GACC) Are Improved by Revised χ Torsions. *J. Phys. Chem. B* **2011**, *115*, 9261−9270.
(39) Zgarbova, M.; Otyepka, M.; Sponer, J.; Mladek, A.; Banas, P.; Cheatham, T. E., III.; Jurecka, P. Refinement of the Cornell et al. Nucleic Acid Force Field Based on Reference Quantum Chemical Calculations of Torsion Profiles of the Glycosidic Torsion. *J. Chem. Theory Comput.* **2011**, *7*, 2886−2902.
(40) Yildirim, I.; Kennedy, S. D.; Stern, H. A.; Hart, J. M.; Kierzek, R.; Turner, D. H. Revision of AMBER Torsional Parameters for RNA Improves Free Energy Predictions for Tetramer Duplexes with GC and iGiC Base Pairs. *J. Chem. Theory Comput.* **2012**, *8*, 172−181.
(41) Chen, A. A.; Garcia, A. E. High-Resolution Reversible Folding of Hyperstable RNA Tetraloops Using Molecular Dynamics Simulations. *Proc. Natl. Acad. Sci. U.S.A.* **2013**, *110*, 16820−16825.
(42) Steinberg, S.; Misch, A.; Sprinzl, M. Compilation of tRNA Sequences and Sequences of tRNA Genes. *Nucleic Acids Res.* **1993**, *21*, 3011−3015.
(43) Grosjean, H.; Sprinzl, M.; Steinberg, S. Post-Transcriptionally Modified Nucleosides in Transfer RNA: Their Locations and Frequencies. *Biochimie* **1995**, *77*, 139−141.
(44) Charette, M.; Gray, M. W. Pseudouridine in RNA: What, Where, How, and Why. *IUBMB Life* **2000**, *49*, 341−351.
(45) Davis, D. R. Biophysical and Conformational Properties of Modified Nucleosides in RNA. In *Modification and Editing of RNA: The Alteration of RNA Structure and Function*; Grosjean, H., Benne, R., Eds.; ASM Press: Washington, DC, 1998; pp 85−102.
(46) Neumann, J. M.; Bernassau, J. M.; Gueron, M.; Tran-Dinh, S. Comparative Conformations of Uridine and Pseudouridine and Their Derivatives. *Eur. J. Biochem.* **1980**, *108*, 457−463.
(47) Davis, D. R.; Veltri, C. A.; Nielsen, L. An RNA Model System for Investigation of Pseudouridine Stabilization of the Codon-Anticodon Interaction in tRNALys, tRNAHis and tRNATyr. *J. Biomol. Struct. Dyn.* **1998**, *15*, 1121−1132.
(48) Eugene, G. M.; Christopher, J. B.; Palenchar, P. M.; Barnhart, L. E.; Paulson, J. L. Identification of a Gene Involved in the Generation of 4-Thiouridine in tRNA. *Nucleic Acids Res.* **1998**, *26*, 2606−2610.
(49) Hruska, F. E.; Ogilvie, K. K.; Smith, A. A.; Wayborn, H. Molecular Conformation of 4-Thiouridine in Aqueous Solution. *Can. J. Chem.* **1971**, *49*, 2449−2452.
(50) Saenger, W.; Scheit, K. H. A Pyrimidine Nucleoside in the SYN Conformation: Molecular and Crystal Structure of 4-Thiouridine-Hydrate. *J. Mol. Biol.* **1970**, *50*, 153−169.
(51) Nasvall, S. J.; Chen, P.; Bjork, G. R. The Modified Wobble Nucleoside Uridine-5-oxyacetic Acid in tRNA$^{Pro}_{cmo}{}^{5}$UGG Promotes Reading of All Four Proline Codons In Vivo. *RNA* **2004**, *10*, 1662−1673.
(52) Vendeix, F. A.; Dziergowska, A.; Gustilo, E. M.; Graham, W. D.; Sproat, B.; Malkiewicz, A.; Agris, P. F. Anticodon Domain Modifications Contribute Order to tRNA for Ribosome-mediated Codon Binding. *Biochemistry* **2008**, *47*, 6117−6129.
(53) Weixlbaumer, A.; Murphy, F. V., IV; Dziergowska, A.; Malkiewicz, A.; Vendeix, F. A. P.; Agris, P. F.; Ramakrishnan, V. Mechanism for Expanding the Decoding Capacity of Transfer RNAs by Modification of Uridines. *Nat. Struct. Mol. Biol.* **2007**, *14*, 498−502.
(54) Yokoyama, S.; Watanabe, T.; Murao, K.; Ishikura, H.; Yamaizumi, Z.; Nishimura, S.; Miyazawa, T. Molecular Mechanism of Codon Recognition by tRNA Species with Modified Uridine in the

First Position of the Anticodon. *Proc. Natl. Acad. Sci. U.S.A.* **1985**, *82*, 4905−4909.
(55) Morikawa, K.; Torii, K.; Iitaka, Y.; Tsuboi, M. Uridine-5-oxyacetic Acid Methyl Ester Monohydrate. *Acta Crystallogr., Sect. B: Struct. Crystallogr. Cryst. Chem.* **1975**, *B31*, 1004−1007.
(56) Case, D. A.; Darden, T. A.; Cheatham, T. E., III.; Simmerling, C. L.; Wang, J.; Duke, R. E.; Luo, R.; Crowley, M.; Walker, R. C.; Zhang, W.; Merz, K. M.; Wang, B.; Hayik, S.; Roitberg, A.; Seabra, G.; Kolossvary, I.; Wong, K. F.; Paesani, F.; Vanicek, J.; Wu, X.; Brozell, S. R.; Steinbrecher, T.; Gohlke, H.; Yang, L.; Tan, C.; Mongan, J.; Hornak, V.; Cui, G.; Mathews, D. H.; Seetin, M. G.; Sagui, C.; Babin, V.; Kollman, P. A. *AMBER 10*; University of California, San Francisco: San Francisco, CA, 2008.
(57) Case, D. A.; Darden, T. A.; Cheatham. T. E., III.; Simmerling, C. L.; Wang, J.; Duke, R. E.; Luo, R.; Walker, R. C.; Zhang, W.; Merz, K. M.; Roberts, B.; Hayik, S.; Roitberg, A.; Seabra, G.; Swails, J.; Goetz, A. W.; Kolossvary, I.; Wong, K. F.; Paesani, F.; Vanicek, J.; Wolf, R. M.; Liu, J.; Wu, X.; Brozell, S. R.; Steinbrecher, T.; Gohlke, H.; Cai, Q.; Ye, X.; Wang, J.; Hsieh, M. J.; Cui, G.; Roe, D. R.; Mathews, D. H.; Seetin, M. G.; Salomon-Ferrer, R.; Sagui, C.; Babin, V.; Luchko, T.; Gusarov, S.; Kovalenko, A.; Kollman, P. A. *AMBER 12*; University of California, San Francisco: San Francisco, CA, 2012.
(58) Jorgensen, W. L.; Chandrasekhar, J.; Madura, J. D.; Impey, R. W.; Klein, M. L. Comparison of Simple Potential Functions for Simulating Liquid Water. *J. Chem. Phys.* **1983**, *79* (2), 926−935.
(59) Wang, J.; Wolf, R. M.; Caldwell, J. W.; Kollman, P. A.; Case, D. A. Development and Testing of a General Amber Force Field. *J. Comput. Chem.* **2004**, *25*, 1157−1175.
(60) Sugita, Y.; Okamoto, Y. Replica-Exchange Molecular Dynamics Method for Protein Folding. *Chem. Phys. Lett.* **1999**, *314*, 141−151.
(61) Ryckaert, J.-P.; Ciccotti, G.; Berendsen, H. J. C. Numerical Integration of the Cartesian Equations of Motion of a System with Constraints: Molecular Dynamics of n-Alkanes. *J. Comput. Phys.* **1977**, *23*, 327−341.
(62) Darden, T.; York, D.; Pedersen, L. Particle Mesh Ewald: An *N*·log(*N*) Method for Ewald Sums in Large Systems. *J. Chem. Phys.* **1993**, *98*, 10089−10092.
(63) Saenger, W. Defining Terms for the Nucleic Acids. In *Principles of Nucleic Acid Structure*; Springer-Verlag: Berlin, Heidelberg, NY, 1984; pp 16−21.
(64) Altona, C.; Sundaralingam, M. Conformational Analysis of the Sugar Ring in Nucleosides and Nucleotides. A New Description Using the Concept of Pseudorotation. *J. Am. Chem. Soc.* **1972**, *94*, 8205−8212.
(65) Denning, E. J.; Priyakumar, U. D.; Nilsson, L.; MacKerell, A. D., Jr. Impact of 2′-Hydroxyl Sampling on the Conformational Properties of RNA: Update of the CHARMM All-atom Additive Force Field for RNA. *J. Comput. Chem.* **2011**, *32*, 1929−1943.
(66) Foloppe, N.; Nilsson, L. Toward a Full Characterization of Nucleic Acid Components in Aqueous Solution: Simulations of Nucleosides. *J. Phys. Chem. B* **2005**, *109*, 9119−9131.
(67) Hart, K.; Foloppe, N.; Baker, C. M; Denning, E. J; Nilsson, L.; Mackerell, A. D., Jr. Optimization of the CHARMM Additive Force Field for DNA: Improved Treatment of the BI/BII Conformational Equilibrium. *J. Chem. Theory Comput.* **2012**, *8*, 348−362.
(68) Foloppe, N.; MacKerell, A. D., Jr. All-Atom Empirical Force Field for Nucleic Acids: 1) Parameter Optimization Based on Small Molecule and Condensed Phase Macromolecular Target Data. *J. Comput. Chem.* **2000**, *21*, 86−104.
(69) Plavec, J.; Thibaudeau, C.; Chattopadhyaya, J. How Do the Energetics of the Stereoelectronic Gauche and Anomeric Effects Modulate the Conformation of Nucleos(t)ides? *Pure Appl. Chem.* **1996**, *68*, 2137−2144.
(70) Dalluge, J. J.; Hashizume, T.; Sopchik, A. E.; McCloskey, J. A.; Davis, D. R. Conformational Flexibility in RNA: The Role of Dihydrouridine. *Nucleic Acids Res.* **1996**, *24*, 1073−1079.
(71) Deslauriers, R.; Lapper, R. D.; Smith, I. C. P. A Proton Magnetic Resonance Study of the Molecular Conformation of a Modified Nucleoside from Transfer RNA. Dihydrouridine. *Can. J. Biochem.* **1971**, *49*, 1279−1284.
(72) Sierzputowska-Gracz, H.; Sochaka, E.; Malkiewicz, A.; Kuo, K.; Gehrke, C. W.; Agris, P. F. Chemistry and Structure of Modified Uridines in the Anticodon Wobble Position of Transfer RNA is Determined by Thiolation. *J. Am. Chem. Soc.* **1987**, *109*, 7171−7177.
(73) Blackburn, B. J.; Grey, A. A.; Smith, I. C. P. Determination of the Molecular Conformation of Uridine in Aqueous Solution by Proton Magnetic Resonance Spectroscopy. Comparison with *β*-pseudouridine. *Can. J. Chem.* **1970**, *48*, 2866−2870.
(74) Okamoto, I.; Cao, S.; Tanaka, H.; Seio, K.; Sekine, M. Synthesis of 4-Thiopseudoisocytidine and 4-Thiopseudouridine as Components of Triplex-Forming Oligonucleotides. *Chem. Lett.* **2009**, *38*, 174−175.
(75) Smith, W. S.; Sierzputowska-Gracz, H.; Sochacka, E.; Malkiewicz, A.; Agris, P. F. Chemistry and Structure of Modified Uridine Dinucleosides Are Determined by Thiolation. *J. Am. Chem. Soc.* **1992**, *114*, 7989−7997.
(76) Agris, P. F.; Sierzputowska-Gracz, H.; Smith, W.; Malkiewicz, A.; Sochacka, E.; Nawrot, B. Thiolation of Uridine Carbon-2 Restricts the Motional Dynamics of the Transfer RNA Wobble Position Nucleoside. *J. Am. Chem. Soc.* **1992**, *114*, 2652−2656.
(77) Rao, S. T.; Sundaralingam, M. Stereochemistry of Nucleic Acids and Their Constituents. 13. The Crystal and Molecular Structure of 3′-O-Acetyladenosine. Conformational Analysis of Nucleosides and Nucleotides with SYN Glycosidic Torsional Angle. *J. Am. Chem. Soc.* **1970**, *92*, 4963−4970.
(78) Altona, C.; Sundaralingam, M. Conformational Analysis of the Sugar Ring in Nucleosides and Nucleotides. Improved Method for the Interpretation of Proton Magnetic Resonance Coupling Constants. *J. Am. Chem. Soc.* **1973**, *95*, 2333−2344.
(79) Yokoyama, S.; Yamaizumi, Z.; Nishimura, S.; Miyazawa, T. ^{1}H NMR Studies on the Conformational Characteristics of 2-Thiopyrimidine Nucleotides Found in Transfer RNAs. *Nucleic Acids Res.* **1979**, *6*, 2611−2626.
(80) Emerson, T. R.; Swan, R. J.; Ulbricht, T. L. V. Optical Rotatory Dispersion of Nucleic Acid Derivatives. VIII. The Conformation of Pyrimidine Nucleosides in Solution. *Biochemistry* **1967**, *6*, 843.
(81) Green, F. A.; Shiono, R.; Rosenstein, R. D.; Abraham, D. J. The X-ray Crystal and Molecular Structure of the Nucleoside *β*-Uridine. *Chem. Commun.* **1971**, *1*, 53−54.
(82) Scheit, K. H.; Saenger, W. The Conformation of 4-Thiouridine-5′-phosphate in Single and Double Stranded Polynucleotides. *FEBS Lett.* **1969**, *2*, 305−308.
(83) Hurd, R. E.; Reid, B. R. NMR Spectroscopy of the Ring Nitrogen Protons of Uracil and Substituted Uracils; Relevance to A Psi Base Pairing in the Solution Structure of Transfer RNA. *Nucleic Acids Res.* **1977**, *4*, 2747−2755.
(84) Altona, C. Conformational Analysis of Nucleic Acids. Determination of Backbone Geometry of Single-Helical RNA and DNA in Aqueous Solution. *Recl. Trav. Chim. Pays-Bas* **1982**, *101*, 413−433.
(85) Orbons, L. P.; Altona, C. Conformational Analysis of the B and Z Forms of the d(m5C-G)3 and d(br5C-G)3 Hexamers in Solution. A 300-MHz and 500-MHz NMR Study. *Eur. J. Biochem.* **1986**, *160*, 141−148.
(86) Sundaralingam, M.; Rao, S. T.; Abola, J. Molecular Conformation of Dihydrouridine: Puckered Base Nucleoside of Transfer RNA. *Science* **1971**, *172*, 725−727.
(87) Saenger, W. Structures and Conformational Properties of Bases, Furanose Sugars, and Phosphate Groups. In *Principles of Nucleic Acid Structure*; Springer-Verlag: Berlin, Heidelberg, NY, 1984; pp 62.
(88) Suck, D.; Saenger, W. Molecular and Crystal Structure of 6-methyluridine. A Pyrimidine Nucleoside in Syn Conformation. *J. Am. Chem. Soc.* **1972**, *94*, 6520−6526.
(89) de Leeuw, H. P. M.; Haasnoot, C. A. G.; Altona, C. Empirical Correlation Between Conformational Parameters in *β*-D-furanoside Fragments Derived from a Statistical Survey of Crystal Structures of Nucleic Acid Constituents. Full Description of Nucleoside Molecular

Geometries in Terms of Four Parameters. *Isr. J. Chem.* **1980**, *20*, 108−126.
(90) Saenger, W. Structures and Conformational Properties of Bases, Furanose Sugars, and Phosphate Groups. In *Principles of Nucleic Acid Structure*; Springer-Verlag: Berlin, Heidelberg, NY, 1984; pp 71−72.
(91) Hruska, F. E. Mapping Nucleoside Conformations in Aqueous Solution. A Correlation of Some Furanose Structural Parameters. In *The Jerusalem Symposia on Quantum Chemistry and Biochemistry. Conformation of Biological Molecules and Polymers*, Proceedings of an International Symposium, Jerusalem, 3−9 April 1972; Bergmann, E. D., Pullman, B., Eds.; Israel Academy of Sciences and Humanities (distributed by Academic Press, New York): Jerusalem, 1973; *5*, pp 345−360.
(92) Zhang, R. b.; Eriksson, L. A. Theoretical Study on Conformational Preferences of Ribose in 2-thiouridine–the Role of the 2′OH Group. *Phys. Chem. Chem. Phys.* **2010**, *12*, 3690−3697.
(93) Saenger, W. Structures and Conformational Properties of Bases, Furanose Sugars, and Phosphate Groups. In *Principles of Nucleic Acid Structure*; Springer-Verlag: Berlin, Heidelberg, NY, 1984; pp 76−77.
(94) Amidon, G. L.; Anik. S.; Rubin. J. An Energy-Partitioning Analysis of Base-Sugar Intramolecular C-H---O Hydrogen Bonding in Nucleosides and Nucleotides. In *Structure and Conformation of Nucleic Acids and Protein-Nucleic Acids Interactions*; Sundaralingam, M., Rao, S. T., Eds.; Univ. Park Press: Baltimore, 1975; pp 729−744.
(95) Saenger, W. Structures and Conformational Properties of Bases, Furanose Sugars, and Phosphate Groups. In *Principles of Nucleic Acid Structure*; Springer-Verlag: Berlin, Heidelberg, NY, 1984; pp 80−81.
(96) Saenger, W. Structures and Conformational Properties of Bases, Furanose Sugars, and Phosphate Groups. In *Principles of Nucleic Acid Structure*; Springer-Verlag: Berlin, Heidelberg, NY, 1984; pp 61−73.